ARTICLE IN PRESS
AESCTE:3022

Aerospace Science and Technology ••• (••••) •••–•••

Contents lists available at ScienceDirect

Aerospace Science and Technology

www.elsevier.com/locate/aescte

Distributed UAV formation control using differential game approach

Wei Lin

Department of EECS, University of Central Florida, Orlando, FL 32816, USA

ARTICLE INFO

Article history:
Received 12 July 2013
Received in revised form 18 January 2014
Accepted 27 February 2014
Available online xxxx

Keywords:
Formation control
Differential games
Distributed control

ABSTRACT

This paper considers a formation control problem for a multiple-UAV (unmanned aerial vehicle) system where each UAV is able to exchange information with other UAVs according to a fixed information graph. In this paper, each UAV tries to minimize its own performance index which is chosen independently based on its local information. Because of the UAVs' different objectives, the formation control problem is formulated and solved as a differential game problem. Realizing the incapability of the classical Nash strategy approach in dealing with the distributed information, we propose a novel open-loop Nash strategy design approach for each UAV to implement in a fully distributed manner through estimating its terminal state. An illustrative example of a five-UAV formation control problem is solved under different scenarios.

1. Introduction

A multiple-UAV (unmanned aerial vehicle) system is often characterized by an environment with physical constraints such that each UAV can only exchange information with neighboring ones. Because of this constraint, the control design for each UAV utilizing only the information available to it becomes a challenge. An important application of this system is the multiple-aircraft (including multi-UAV) formation control problem which is to design control inputs such that a prescribed formation is formed among the aircrafts. In recent years, a variety of results on aircraft formation control have emerged. Some of them are reviewed as follows. In [21], the decentralized overlapping control was design to control a group of interconnected UAVs, where a feedback controller was designed in the expanded space for each UAV and then converted back to the original space. In [7], the aerodynamics coupling effects of the formation flying system was studied and the trajectory tracking control and formation keeping control were combined and designed using linear quadratic regulator approach. In [10], the high-level formation control problem of organic air vehicles (OAVs) was considered using receding horizon control approach. In [22], a unified optimal control approach including formation control, trajectory tracking, and obstacle avoidance was proposed for multiple-UAV coordination. In [23], the fuel optimization of formation initialization problem for spacecraft was considered and the optimization was convexified and solved as a semidefinite program. In [11], the attitude synchronization problem of the spacecraft was considered and the decentralized control algorithm was developed based on nonlinear cooperative control theory. A comprehensive review in larger scope on multi-agent control systems including recent progress on aircraft formation control can be found in [6]. Most of the recent results on formation control problem utilize tools such as cooperative control theory [17,16], optimal control theory [5,2], receding horizon control [15,4], etc., and all the aircrafts are usually assumed to pursue a common goal of minimizing the total formation errors and velocity differences among them. However, it is of practical interest to have a more general setting where individual aircrafts can have their own objectives. For example, one aircraft's objectives might be chosen based on its locally measured formation errors and velocity differences. Therefore, given the aircrafts' different objectives, the formation control problem indeed becomes a differential game problem [9]. However, only a few research works have been done in this area. In [8], the formation control problem was formulated as a noncooperative differential game and the receding horizon Nash equilibrium was solved. In [18], the consensus problem as a special case of formation control problem was formulated as a cooperative differential game and the Nash bargain solution among the Pareto-efficient solutions was found using linear matrix inequality (LMI) approach. In this paper, based on the previous results, we consider the distributed Nash strategy design approach for multiple-UAV formation control problem. We will propose a novel approach that enables each UAV to implement its Nash strategy only based on the information available to it only.

The rest of the paper is organized as follows: The problem is formulated in Section 2. We derive the classical open-loop Nash equilibrium in Section 3. The distributed Nash strategy design approach is provided in Section 4. An illustrative example of

E-mail address: weilin0929@gmail.com.

http://dx.doi.org/10.1016/j.ast.2014.02.004

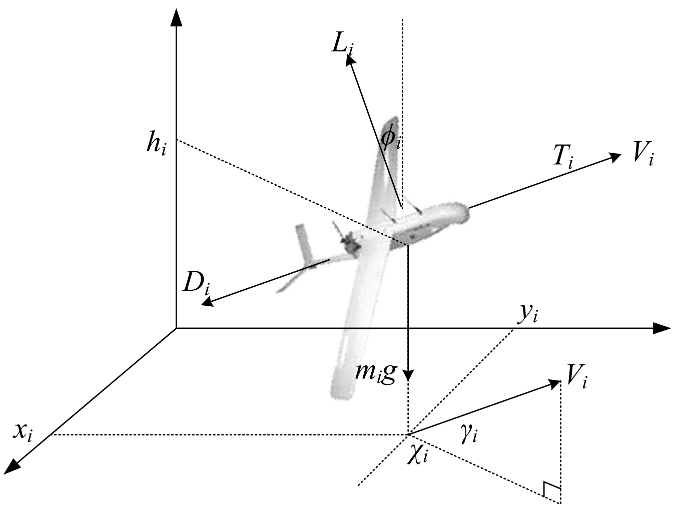

Fig. 1. UAV model.

a five-UAV formation control problem is solved in Section 5. The paper is concluded in Section 6.

2. Problem formulation

2.1. UAV model

Since there exist various UAVs that are designed to complete different real life tasks, it is impossible to have one universal mathematical dynamic model to describe all the UAVs. This paper only focuses on the high-level formation control design among a group of UAVs and hence will adopt a representative UAV model which has been commonly used in many literatures [13,16,22]. We consider a system of N UAVs with the following point-mass model [13] as shown in Fig. 1:

$$\dot{x}_i = V_i \cos\gamma_i \cos\chi_i, \tag{1}$$

$$\dot{y}_i = V_i \cos\gamma_i \sin\chi_i \tag{2}$$

$$\dot{h}_i = V \sin\gamma_i \tag{3}$$

$$\dot{V}_i = \frac{T_i - D_i}{m_i} - g\sin\gamma_i \tag{4}$$

$$\dot{\gamma}_i = \frac{L\cos\Phi_i - m_i g\cos\gamma_i}{m_i V_i} \tag{5}$$

$$\dot{\chi}_i = \frac{L_i \sin\Phi_i}{m_i V_i \cos\gamma_i} \tag{6}$$

for $i = 1, \ldots, N$, where x_i is the down-range displacement, y_i is the cross-range displacement, h_i is the altitude, V_i is the ground speed which is assumed to be equal to the airspeed in this paper, γ_i is the flight path angle, χ_i is the heading angle, T_i is the engine thrust, D_i is the drag, m_i is the UAV mass, g is the acceleration due to gravity, L_i is the lift, and Φ_i is the banking angle. The three control inputs of UAV i is the banking angle Φ_i, lift L_i, and engine thrust T_i.

It is shown in [13] that the highly nonlinear UAV model in (2.1) can be pre-linearized using feedback linearization to be

$$\ddot{x}_i = u_{xi}, \qquad \ddot{y}_i = u_{yi}, \qquad \ddot{h}_i = u_{hi} \tag{7}$$

where u_{xi}, u_{yi}, and u_{hi} are the virtual acceleration control inputs. These virtual control inputs and the real control inputs are related through the following equations

$$\Phi_i = \tan^{-1}\left(\frac{u_{yi}\cos\chi_i - u_{xi}\sin\chi_i}{(u_{hi}+g)\cos\gamma_i - (u_{xi}\cos\chi_i + u_{yi}\sin\chi_i)\sin\gamma_i}\right) \tag{8}$$

$$L_i = m_i \frac{(u_{hi}+g)\cos\gamma_i - (u_{xi}\cos\chi_i + u_{yi}\sin\chi_i)\sin\gamma_i}{\cos\Phi_i} \tag{9}$$

$$T_i = m_i\big[(u_{hi}+g)\sin\gamma_i + (u_{xi}\cos\chi_i + u_{yi}\sin\chi_i)\cos\gamma_i\big] + D_i \tag{10}$$

where $\tan\chi_i = \dot{y}_i/\dot{x}_i$ and $\sin\gamma_i = \dot{h}_i/V_i$. Therefore, after the virtual control inputs are designed based on the linear model (7), the real control inputs can then be obtained by substituting the virtual ones into (7). Expressing (7) in terms of state-space representation yields

$$\dot{z}_i = Az_i + Bu_i, \tag{11}$$

$$p_i = C_p z_i \tag{12}$$

$$v_i = C_v z_i \tag{13}$$

where $z_i = [p_i^T \ \ v_i]^T$ is the state vector, p_i is the position vector, v_i is the velocity vector, $u_i = [u_{xi}^T \ \ u_{yi}^T \ \ u_{hi}^T]^T$ is the virtual acceleration control vector,

$$A_i = \begin{bmatrix} 0 & 1 \\ 0 & 0 \end{bmatrix} \otimes I_3, \qquad B_i = \begin{bmatrix} 0 \\ 1 \end{bmatrix} \otimes I_3,$$

$$C_p = [1 \quad 0] \otimes I_3, \qquad C_v = [0 \quad 1] \otimes I_3,$$

$I_3 \in \mathbb{R}^{3\times 3}$ is the identity matrix, and $\otimes$ is the Kronecker product.

2.2. Information graph

Suppose that individual UAVs are able to communicate with each other in a certain pattern to achieve the desired formation. We define a time-invariant directed information graph $\mathcal{G} = (\mathcal{V}, \mathcal{E})$ to describe the information exchange pattern among them. Specifically, node $v_i \in \mathcal{V}$ represents UAV i and edge $e_{ij} \in \mathcal{E}$ represents the directional information transmission from UAV j to UAV i. Several terminologies from graph theory are introduced as follows.

Definition 1. Node i is globally reachable in graph $\mathcal{G}$ if there exists a sequence of edges directed from v_i to v_j for all $j = 1, \ldots, N$, $j \neq i$.

A globally reachable node is also known as a root node of a spanning tree on the graph. Based on the definition of globally reachable node, the connectivity of a graph is defined as follows.

Definition 2. Graph $\mathcal{G}$ is connected if there exists at least one globally reachable node.

In this paper, to achieve the formation requirement, the connectivity of the UAVs on the information graph must be assured. Hence, we make the following assumption:

Assumption 1. The underlying information graph among the N UAVs is connected.

A widely used mathematical tool in graph theory is the Laplacian matrix $\mathcal{L} = [\mathcal{L}_{ij}] \in \mathbb{R}^{N\times N}$ which is defined as follows:

$$\mathcal{L}_{ij} = \begin{cases} -l_{ij} & \text{if } e_{ij} \in \mathcal{E} \text{ for } j \neq i \\ 0 & \text{if } e_{ij} \notin \mathcal{E} \text{ for } j \neq i \\ -\sum_{q=1,\, q\neq i}^{N} l_{iq} & \text{if } j = i, \end{cases} \tag{14}$$

Please cite this article in press as: W. Lin, Distributed UAV formation control using differential game approach, Aerospace Science and Technology (2014), http://dx.doi.org/10.1016/j.ast.2014.02.004

where l_{ij} is a positive scalar represents the weight made by UAV i on the information transmitted through $e_{ij} \in \mathcal{E}$. In this paper, scalar l_{ij} can be regarded as a weighting factor of UAV i's willingness to keep the desired displacement between itself and UAV j for $e_{ij} \in \mathcal{E}$. A larger weight indicates a stronger willingness. Furthermore, a well known property of the Laplacian matrix is that all its eigenvalues always have nonnegative real parts.

2.3. Performance indices and Nash equilibrium

The objective of this paper is to design control inputs for individual UAVs to form a prescribed formation. Hence, assuming that the desired displacement vector pointing from UAV j to UAV i is α_{ij}, the formation requirement can be expressed mathematically in terms of the following performance index for UAV i to minimize:

$$J_i = \sum_{e_{ij} \in \mathcal{E}} \frac{l_{ij}}{2} \left[\left\| p_i(t_f) - p_j(t_f) - \alpha_{ij} \right\|^2 + \left\| v_i(t_f) - v_j(t_f) \right\|^2 \right] + \frac{r_i}{2} \int_0^{t_f} \|u_i\|^2 \, dt \quad \forall i = 1, \dots, N, \tag{15}$$

where $\|\cdot\|$ is the Euclidean norm, l_{ij} is the entry of the Laplacian matrix defined in (14), and r_i is a positive scalar, $t_f > 0$ is the terminal time. Performance index (15) means that UAV i will try to minimize a weighted sum of the terminal formation errors and velocity errors according to the information graph while at the same time minimizing its control effort made during the entire formation control process. The coefficients in the performance index (15) represent the penalties on the terminal formation errors, velocity errors, and control effort. The larger the coefficients are, the more emphases are placed on the corresponding terms. Note that coefficients l_{ij} and r_i in performance index (15) for different UAVs are not necessarily the same because these coefficients reflect the real situation. For instance, if UAV i has sufficient fuel in its tank, it will naturally choose a large value of l_{ij} and a small value of r_i in order to keep the desired formation with others actively. On the contrary, if UAV i does not have much fuel left in its tank, it will naturally choose a small value of l_{ij} and a large value of r_i to preserve its energy or fuel cost. Therefore, since there exist different performance indices for the N UAVs, the formation control problem in fact becomes a differential game problem. In this paper, we consider the Nash equilibrium solution for this game problem and the definition of Nash equilibrium is as follows: For the N-UAV differential game defined by system (11)–(13) and performance indices described in (15), the strategies $u_1^*, \dots, u_N^*$ form a Nash equilibrium if

$$J_i(u_1^*, \dots, u_N^*) \leqslant J_i(u_1^*, \dots, u_{i-1}^*, u_i, u_{i+1}^*, \dots, u_N^*) \quad \forall u_i \in U_i \tag{16}$$

hold for all $i = 1, \dots, N$, where U_i is UAV i's admissible strategy set.

In other words, once the UAVs' strategy form a Nash equilibrium, no one tends to deviate from the Nash equilibrium unilaterally. To derive the Nash equilibrium, the admissible strategy set U_i must be clearly specified and it is closely related with the information structure [3]. In this paper, we will seek the open-loop Nash equilibrium for the UAVs where UAV i's admissible strategy set U_i contains strategy as a function of the initial states $z_1(0), \dots, z_N(0)$ and t only.

3. Classical open-loop Nash equilibrium

In this section, the open-loop Nash equilibrium for the formulated differential game is derived. To begin with, we define the following new state vectors to simplify the problem:

$$s_{pi}(t) = [1 \quad t_f - t] z_i(t) \quad \text{and} \quad s_{vi}(t) = [0 \quad 1] z_i(t). \tag{17}$$

Differentiating both sides of (17) with respect to t and recalling system dynamics (11)–(13) yield

$$\dot{s}_{pi} = \tilde{B}_p u_i \quad \text{and} \quad \dot{s}_{vi} = \tilde{B}_v u_i, \tag{18}$$

where $\tilde{B}_p = (t_f - t) I_3$ and $\tilde{B}_v = I_3$. Based on the properties $s_{pi}(t_f) = p_i(t_f)$ and $s_{vi}(t_f) = v_i(t_f)$ for s_{pi} and s_{vi} defined in (17), the performance indices in (15) can be rewritten as

$$J_i = \sum_{e_{ij} \in \mathcal{E}} \frac{l_{ij}}{2} \left[\left\| s_{pi}(t_f) - s_{pj}(t_f) - \alpha_{ij} \right\|^2 + \left\| s_{vi}(t_f) - s_{vj}(t_f) \right\|^2 \right] + \frac{r_i}{2} \int_0^{t_f} \|u_i\|^2 \, dt \quad \forall i = 1, \dots, N. \tag{19}$$

Before we present the result of open-loop Nash equilibrium, the following lemma is introduced first.

Lemma 1. *All the eigenvalues of matrix M defined by*

$$M = \left[I_{2N} + W \otimes \left(R^{-1} \mathcal{L} \right) \right] \otimes I_3, \tag{20}$$

have positive real parts, where $\mathcal{L}$ is the graph Laplacian matrix defined in (14),

$$W = \begin{bmatrix} w_{pp} & w_{pv} \\ w_{vp} & w_{vv} \end{bmatrix}, \tag{21}$$

$$w_{pp} = \int_0^{t_f} \tilde{B}_p \tilde{B}_p^T \, dt = \frac{t_f^3}{3}, \qquad w_{pv} = \int_0^{t_f} \tilde{B}_p \tilde{B}_v^T \, dt = \frac{t_f^2}{2} \tag{22}$$

$$w_{vp} = \int_0^{t_f} \tilde{B}_v \tilde{B}_p^T \, dt = \frac{t_f^2}{2}, \qquad w_{vv} = \int_0^{t_f} \tilde{B}_v \tilde{B}_v^T \, dt = t_f, \tag{23}$$

$$R = \operatorname{diag}\{r_1, \dots, r_N\}, \tag{24}$$

and diag$\{\cdot\}$ *stands for "diagonal matrix".*

Proof. Firstly, since matrix W is obviously positive define, all its eigenvalues are positive. Secondly, since matrix R in (24) is a positive diagonal matrix, the product of $(R^{-1}\mathcal{L})$ becomes a new weighted Laplacian matrix whose eigenvalues still have nonnegative real parts. Thirdly, since the eigenvalues of matrices' Kronecker product are the product of these matrices' eigenvalues, all the eigenvalues of matrix $[W \otimes (R^{-1}\mathcal{L})]$ have nonnegative real parts. Therefore, all the eigenvalues of M in (20) have positive real parts. □

The open-loop Nash equilibrium solution is now presented as follows.

Theorem 1. *Given the differential game among N UAVs with system dynamics (18) and performance indices (19), the strategies*

$$u_i^* = -\frac{1}{r_i} F_i M^{-1} \left(\begin{bmatrix} s_p(0) \\ s_v(0) \end{bmatrix} + W_\alpha \alpha \right) + \frac{1}{r_i} \tilde{B}_p^T \alpha_i \quad \forall i = 1, \dots, N \tag{25}$$

form an open-loop Nash equilibrium, where matrix M is defined in (20),

$$s_p = \begin{bmatrix} s_{p1}^T & \cdots & s_{pN}^T \end{bmatrix}^T, \qquad s_v = \begin{bmatrix} s_{v1}^T & \cdots & s_{vN}^T \end{bmatrix}^T, \tag{26}$$

$$F_i = \begin{bmatrix} \tilde{B}_p^T & \tilde{B}_v^T \end{bmatrix}\begin{bmatrix} I_2 \otimes (d_i^T \mathcal{L}) \otimes I_3 \end{bmatrix}, \tag{27}$$

$$W_\alpha = \begin{bmatrix} w_{pp} \\ w_{vp} \end{bmatrix} \otimes R^{-1} \otimes I_3, \tag{28}$$

$$\alpha = \begin{bmatrix} \alpha_1^T & \cdots & \alpha_N^T \end{bmatrix}^T, \tag{29}$$

$$\alpha_i = \sum_{e_{ij}\in\mathcal{E}} l_{ij}\alpha_{ij} \quad \forall i = 1, \ldots, N, \tag{30}$$

$\mathcal{L}$ is the Laplacian matrix defined in (14), $d_i \in \mathbb{R}^N$ is a vector with the ith entry equal to 1 and the other entries equal to 0, and scalars w_{pp} and w_{vp} are defined in (22) and (23), respectively.

Proof. We define the Hamiltonian for UAV i as

$$H_i = \frac{r_i}{2}\|u_i\|^2 + \lambda_{pi}^T \tilde{B}_p u_i + \lambda_{vi}^T \tilde{B}_v u_i$$

where vectors λ_{pi} and λ_{vi} are the Lagrangian multipliers. According to the well known Pontryagin's minimum principle [14], the necessary conditions for optimality are

$$\dot{s}_{pi} = \frac{\partial H_i}{\partial \lambda_{pi}} = \tilde{B}_p u_i, \qquad \dot{s}_{vi} = \frac{\partial H_i}{\partial \lambda_{vi}} = \tilde{B}_v u_i \tag{31}$$

$$\dot{\lambda}_{pi} = -\frac{\partial H_i}{\partial s_{pi}} = 0, \qquad \dot{\lambda}_{vi} = -\frac{\partial H_i}{\partial s_{vi}} = 0, \tag{32}$$

$$\lambda_{pi}(t_f) = \sum_{e_{ij}\in\mathcal{E}} l_{ij}\begin{bmatrix} s_{pi}(t_f) - s_{pj}(t_f) - \alpha_{ij} \end{bmatrix}, \tag{33}$$

$$\lambda_{vi}(t_f) = \sum_{e_{ij}\in\mathcal{E}} l_{ij}\begin{bmatrix} s_{vi}(t_f) - s_{vj}(t_f) \end{bmatrix}, \tag{34}$$

$$\frac{\partial H_i}{\partial u_i} = r_i u_i + \tilde{B}_p^T \lambda_{pi} + \tilde{B}_v^T \lambda_{vi} = 0, \qquad \frac{\partial^2 H_i}{\partial u_i^2} = r_i > 0. \tag{35}$$

Conditions (32)–(34) indicate that λ_{pi} and λ_{vi} are constant vectors. Substituting them into (35) yields

$$\begin{aligned} u_i &= -\frac{1}{r_i}\tilde{B}_p^T \lambda_{pi} - \frac{1}{r_i}\tilde{B}_v^T \lambda_{vi} \\ &= -\frac{1}{r_i}\tilde{B}_p^T \sum_{e_{ij}\in\mathcal{E}} l_{ij}\begin{bmatrix} s_{pi}(t_f) - s_{pj}(t_f) - \alpha_{ij} \end{bmatrix} \\ &\quad - \frac{1}{r_i}\tilde{B}_v^T \sum_{e_{ij}\in\mathcal{E}} l_{ij}\begin{bmatrix} s_{vi}(t_f) - s_{vj}(t_f) \end{bmatrix}. \end{aligned} \tag{36}$$

Substituting (36) into (31) and integrating both sides from 0 to t_f yield

$$\begin{aligned} &s_{pi}(t_f) + \frac{w_{pp}}{r_i}\sum_{e_{ij}\in\mathcal{E}} l_{ij}\begin{bmatrix} s_{pi}(t_f) - s_{pj}(t_f) \end{bmatrix} \\ &\quad + \frac{w_{pv}}{r_i}\sum_{e_{ij}\in\mathcal{E}} l_{ij}\begin{bmatrix} s_{vi}(t_f) - s_{vj}(t_f) \end{bmatrix} = s_{pi}(0) + \frac{w_{pp}}{r_i}\alpha_i \end{aligned} \tag{37}$$

And

$$\begin{aligned} &s_{vi}(t_f) + \frac{w_{vp}}{r_i}\sum_{e_{ij}\in\mathcal{E}} l_{ij}\begin{bmatrix} s_{pi}(t_f) - s_{pj}(t_f) \end{bmatrix} \\ &\quad + \frac{w_{vv}}{r_i}\sum_{e_{ij}\in\mathcal{E}} l_{ij}\begin{bmatrix} s_{vi}(t_f) - s_{vj}(t_f) \end{bmatrix} = s_{vi}(0) + \frac{w_{vp}}{r_i}\alpha_i \end{aligned} \tag{38}$$

where scalars w_{pp}, w_{pv}, w_{vp}, w_{vv} are defined in (22)–(23) and α_i is defined in (30). Combining (37) and (38) and stacking them from $i = 1$ to $i = N$ yield

$$\begin{bmatrix} s_p(t_f) \\ s_v(t_f) \end{bmatrix} = M^{-1}\left\{\begin{bmatrix} s_p(0) \\ s_v(0) \end{bmatrix} + \left(\begin{bmatrix} w_{pp} \\ w_{vp} \end{bmatrix} \otimes R^{-1} \otimes I_3\right)\alpha\right\} \tag{39}$$

where vectors s_p and s_v are defined in (26), matrix M is defined in (20) and invertible according to Lemma 1, and vector α is defined in (29). Therefore, rewriting (36) as

$$u_i = -\frac{1}{r_i}F_i\begin{bmatrix} s_p(t_f) \\ s_v(t_f) \end{bmatrix} + \frac{1}{r_i}\tilde{B}_p^T \alpha_i \tag{40}$$

where F_i is defined in (27) and substituting (39) into (40) yields (25). Since $s_p(0)$, $s_v(0)$ are in fact functions of the initial state $z(0)$ through (17), strategies $u_1^*, \ldots, u_N^*$ in (25) form an open-loop Nash equilibrium. □

Note that since M^{-1} is generally a full matrix, implementing open-loop Nash strategies in (25) requires individual UAVs to have the knowledge of $s_p(0)$ and $s_v(0)$. However, since UAV i is only able to receive information from UAV j for $e_{ij}\in\mathcal{E}$, vectors $s_p(0)$ and $s_v(0)$ containing global initial state information are generally not available to individual UAVs. Hence, the open-loop Nash strategy u_i^* in (25) is generally not implementable unless the underlying information graph of the N UAVs is fully connected. Therefore, to overcome the difficulty of implementing these Nash strategies, an appropriate Nash strategy design approach must be proposed for individual UAVs in a distributed manner, that is, each UAV can carry out the approach with the information available to it only. This design objective leads to the following section.

4. Nash strategies design in a distributed manner

Realizing that the Nash strategy design approach in the previous section is unable to meet the information transmission requirement on the graph, we propose a novel Nash strategy design approach in a distributed manner in this section. Firstly, note that although the Nash strategy u_i^* in (25) is not directly implementable, its equivalent expression in (36) is indeed in the distributed manner if UAV i is able to figure out its own terminal position $s_{pi}(t_f) = p_i(t_f)$ and terminal velocity $s_{vi}(t_f) = v_i(t_f)$ as well as UAV j's terminal position $s_{pj}(t_f) = p_j(t_f)$ and terminal velocity $s_{vj}(t_f) = v_j(t_f)$ for $e_{ij}\in\mathcal{E}$. Because of this distributed structure in (36), the problem really reduces down to proposing a distributed estimation approach such that each UAV is able to estimate its own terminal position and terminal velocity while at the same time exchanging these estimations with other UAVs according to the information graph. Toward that end, we have the following result.

Theorem 2. *If UAV i updates its terminal position estimate h_{pi} and terminal velocity estimate h_{vi} in continuously in time from any initial guess $h_{pi}(0)$ and $h_{vi}(0)$ according to*

$$\begin{aligned} \begin{bmatrix} \dot{h}_{pi} \\ \dot{h}_{vi} \end{bmatrix} = k_i\Bigg\{&\begin{bmatrix} s_{pi}(0) \\ s_{vi}(0) \end{bmatrix} + \frac{1}{r_i}\begin{bmatrix} w_{pp} \\ w_{vp} \end{bmatrix}\alpha_i - \begin{bmatrix} h_{pi} \\ h_{vi} \end{bmatrix} \\ &- \frac{1}{r_i}(W \otimes I_3)\sum_{e_{ij}\in\mathcal{E}} l_{ij}\left(\begin{bmatrix} h_{pi} \\ h_{vi} \end{bmatrix} - \begin{bmatrix} h_{pj} \\ h_{vj} \end{bmatrix}\right)\Bigg\} \end{aligned} \tag{41}$$

where k_i is a positive scalar, matrix W is defined in (21), and vector α_i is defined in (30), then

$$\lim_{\tau\to\infty}\begin{bmatrix} h_p(\tau) \\ h_v(\tau) \end{bmatrix} = \begin{bmatrix} s_p(t_f) \\ s_v(t_f) \end{bmatrix}, \tag{42}$$

where $h_p = [h_{p1}^T \ \cdots \ h_{pN}^T]^T$, $h_v = [h_{v1}^T \ \cdots \ h_{vN}^T]^T$, and vectors $s_p(t_f)$ and $s_v(t_f)$ are UAVs' terminal positions and terminal velocities as defined in (39).

Proof. Stacking Eq. (41) from $i=1$ to $i=N$ yields

$$\begin{bmatrix} \dot{h}_p \\ \dot{h}_v \end{bmatrix} = K\left\{\begin{bmatrix} s_p(0) \\ s_v(0) \end{bmatrix} - M\begin{bmatrix} h_p \\ h_v \end{bmatrix} + W_\alpha \alpha\right\}, \tag{43}$$

where $K = I_2 \otimes \operatorname{diag}\{k_1, \dots, k_N\} \otimes I_3$, matrix M is defined in (20), matrix W_α is defined in (28), and vector α is defined in (29). Since all the eigenvalues of matrix M have positive real parts as shown in Lemma 1, matrix $(-M)$ is Hurwitz. Therefore, linear system with respect to $[h_p; h_v]$ in (43) is asymptotically stable starting from any initial condition $h(0)$ and will converge to the equilibrium, i.e.,

$$\lim_{\tau\to\infty}\begin{bmatrix} h_p(\tau) \\ h_v(\tau) \end{bmatrix} = M^{-1}\left\{\begin{bmatrix} s_p(0) \\ s_v(0) \end{bmatrix} + W_\alpha \alpha\right\},$$

where the right hand side of the above equation is equal to the vector $[s_p(t_f); s_v(t_f)]$ defined in (39). Therefore, Eq. (42) holds. □

Using the estimation law in (41), individual UAVs are able to asymptotically estimate their terminal positions and terminal velocities by exchanging their estimates according to the graph. Note that the proposed estimation law (41) is fully distributed in the sense that in order to implement it, UAV i only needs to

- **retain** its private information, k_i, $s_{pi}(0)$, $s_{vi}(0)$, l_{ij}, α_i,
- **receive** the terminal state estimate(s) h_j from UAV j for all $e_{ij} \in \mathcal{E}$, $j = 1, \dots, N$, and
- **send** its terminal state estimate h_i to UAV j if $e_{ji} \in \mathcal{E}$, $j = 1, \dots, N$.

Given the distributed state estimation law (41), one possible way to implement the open-loop Nash strategy is to let all the agents in the system communicate for a while until satisfactory convergent values, say $\hat{h}_{pi}$ and $\hat{h}_{vi}$, are reached before the game starts and the UAVs will then implement the open-loop Nash strategy expressed in (36) with $s_{pi}(t_f)$ and $s_{vi}(t_f)$ with $\hat{h}_{pi}$ and $\hat{h}_{vi}$. Such a design approach can be regarded as an offline computation approach. Although the offline approach provides an accurate enough strategy design, it may not be suitable for the situation where the real-time implementation is required. This can be achieved by using the following real-time implementation algorithm:

$$\begin{aligned}\begin{bmatrix} \dot{h}_{pi} \\ \dot{h}_{vi} \end{bmatrix} = k_i\Bigg\{&\begin{bmatrix} s_{pi}(0) \\ s_{vi}(0) \end{bmatrix} + \frac{1}{r_i}\left(\begin{bmatrix} w_{pp} \\ w_{vp} \end{bmatrix} \otimes I_3\right)\alpha_i \\ &- \begin{bmatrix} h_{pi} \\ h_{vi} \end{bmatrix} - \frac{1}{r_i}(W \otimes I_3) \\ &\times \sum_{e_{ij}\in\mathcal{E}} l_{ij}\left(\begin{bmatrix} h_{pi} \\ h_{vi} \end{bmatrix} - \begin{bmatrix} h_{pj} \\ h_{vj} \end{bmatrix}\right)\Bigg\},\end{aligned} \tag{44}$$

$$u_i^* = -\frac{1}{r_i}\tilde{B}_p^T \sum_{e_{ij}\in\mathcal{E}} l_{ij}(h_{pi} - h_{pj} - \alpha_{ij}) - \frac{1}{r_i}\tilde{B}_v^T \sum_{e_{ij}\in\mathcal{E}} l_{ij}(h_{vi} - h_{vj}), \tag{45}$$

where Eq. (44) is the terminal state estimation law and Eq. (45) is the open-loop Nash control using the terminal estimates directly. Therefore, for either offline or real-time implementation, individual UAVs are able to implement the open-loop Nash strategies in a distributed manner by measuring and calculating the initial states $s_1(0), \dots, s_N(0)$ and exchanging the terminal position estimates and terminal velocity estimates among themselves according to the graph. Since it is better to have the estimation law converge fast, one can choose a large positive scalar g_i to achieve satisfactory convergence speed.

Remark 1. One important feature of the proposed design is that to implement it, each UAV does not need to have the knowledge of the other UAVs' performance indices. This feature could be significant in the real life controller design because as we mentioned earlier, individual UAVs choose their coefficients of their performance indices in (15) independently based on their weights on a variety of factors, such as local formation errors, local velocity errors, and the amount of fuel left in their tanks. Moreover, each UAV is usually not able to know the overall information graph among all the UAVs. Therefore, the distributed strategy design in (43) conforms with the aforementioned real application constraints.

Remark 2. Although the proposed design approach is derived based on the virtual double-integrator dynamics (11), the approach can be in fact easily extended to the case where the UAVs have heterogeneous linear time-varying systems. For more details on the general case, please refer to [12].

Remark 3. As we know, the feedback control structure rather than the open-loop control structure is preferred in many applications because it can react instantaneously to the change of the system. To make the proposed Nash strategy design approach more adaptive to the unexpected changes in the system including the case where the information topology is changing over time, we can utilize the sampled-Nash approach [19]. Toward that end, instead of (15), we can consider the following performance indices

$$\begin{aligned} J_i(t_k) = \sum_{e_{ij}\in\mathcal{E}} \frac{l_{ij}}{2}\Big[\big\|p_i(t_f) - p_j(t_f) - \alpha_{ij}\big\|^2 + \big\|v_i(t_f) - v_j(t_f)\big\|^2\Big] \\ + \frac{r_i}{2}\int_{tk}^{t_f} \|u_i\|^2\, dt \quad \forall k = 1, \dots, N_s \end{aligned} \tag{46}$$

where $0 = t_1 \leqslant t_2 \leqslant \cdots \leqslant t_{Ns} = t_f$. Hence, based on (43), the sampled distributed Nash strategy design algorithm is proposed as follows.

Algorithm 1. At $t = t_k$,

1. UAV i measures and calculates $s_{pi}(t_k)$ and $s_{vi}(t_k)$ for $i = 1, \dots, N$.
2. UAV i implements (43) with $[s_{pi}(0); s_{vi}(0)]$ replaced by $[s_{pi}(t_k); s_{vi}(t_k)]$ and

$$w_{pp} = \frac{(t_f - t_k)^3}{3}, \qquad w_{pv} = w_{vp} = \frac{(t_f - t_k)^2}{2},$$
$$w_{vv} = t_f - t_k$$

   for $i = 1, \dots, N$.
3. Once $t = t_{k+1}$ arrives, the UAVs repeat the steps 1 and 2 by letting $t_k \to t_{k+1}$.

As we can see from the above algorithm, the UAVs measure the state variables multiple times during the process and will hence be more aware of the change in the system. Based on this sampled-Nash approach, we are able to consider the Nash strategies design under time-varying information topology which might occur due to communication failure or obstacles etc. We denote $\mathcal{G}(t) = \{\mathcal{V}, \mathcal{E}(t)\}$ as the time-varying graph. If we assume that the time interval between two consecutive sample instants t_k and t_{k+1}

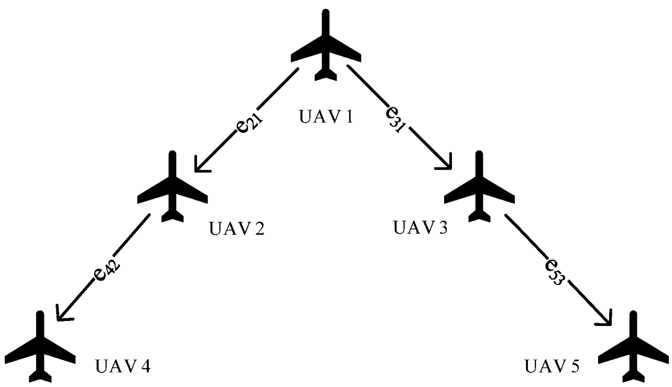

Fig. 2. Triangle formation shape and information graph.

is small enough such that the information topology remains the same within the interval, then the UAVs are subject performance indices in (46) with $\mathcal{E}$ replaced by $\mathcal{E}(t_k)$. Essentially, every UAV only needs to adjust its performance index according to the information graph every time its local communication pattern changes. In this case, the terminal state estimation algorithm should still be applicable with minor changes. Once there is a change in the information graph, the equation will have a different equilibrium. Since the algorithm is always fully distributed and asymptotically stable, all the players will quickly reach a stable terminal state estimate after communicate for a while according to the information graph and hence the new Nash strategies are obtained. More property on the switching topology is still under investigation.

5. Illustrative example and simulation results

In this section, we consider a formation problem of a five-UAV system to illustrate the proposed distributed Nash formation control design approach. The parameters in [22] are utilized for this simulation: The weight of UAV i is $m_i = 20$ kg for all $i = 1, \dots, N$. The gravity constant is $g = 9.81$ kg/m^2. The drag D_i is calculated as follows [24]:

$$D_i = \frac{0.5\rho(V_i - V_{wi})^2 S C_{D0} + 2k_d k_n^2 L^2/g^2}{\rho(V_i - V_{wi})^2 S}$$

where ρ is the atmospheric density and equal to 1.225 kg/m^3, V_{wi} is the gust, S is the wing area and equal to 1.37 m^2, C_{D0} is the zero-lift drag coefficient and equal to 0.02, k_d is the induced drag coefficient and equal to 0.1, and k_n is the load-factor effectiveness and equal to 1. The gust V_{wi} is modeled as follows [1]:

$$V_{wi} = \bar{V}_{wi} + \delta V_{wi}$$

$$\bar{V}_{wi} = 0.215 V_m \log_{10}(h_i) + 0.285 V_m$$

where $\bar{V}_{wi}$ is the normal wind shear, V_m is the mean wind speed and equal to 4 m/s at the altitude of 80 m, and δV_{wi} is the wind gust turbulence on UAV i and assumed to be a Gaussian random variable with zero mean and a standard deviation equal to $0.09V_m$. The real control inputs of the UAV have the following constraints: $T_i < 125N$, $-294.3N < L_i < 392.4N$, and $-80° \leqslant \Phi_i \leqslant 80°$ for all $i = 1, \dots, N$.

The UAVs are trying to form a desired V-shape in the same altitude shown in Fig. 2 and the underlying directed information graph is also shown in this figure where we can see that UAV 1 is the globally reachable node and is regarded as the leader who only sends out its information but not receives any information. Hence, UAV 1 will act as a reference for the other UAVs. The corresponding graph Laplacian matrix is

$$L = \begin{bmatrix} 0 & 0 & 0 & 0 & 0 \\ -a_{21} & a_{21} & 0 & 0 & 0 \\ -a_{31} & 0 & a_{31} & 0 & 0 \\ 0 & -a_{42} & 0 & a_{42} & 0 \\ 0 & 0 & -a_{53} & 0 & a_{53} \end{bmatrix}.$$

The desired offset vectors of the formation among the UAVs are

$$\alpha_{21} = \begin{bmatrix} -100 \\ -100 \\ 0 \end{bmatrix} \text{m}, \qquad \alpha_{31} = \begin{bmatrix} 100 \\ -100 \\ 0 \end{bmatrix} \text{m},$$

$$\alpha_{42} = \begin{bmatrix} -100 \\ -100 \\ 0 \end{bmatrix} \text{m}, \qquad \alpha_{53} = \begin{bmatrix} 100 \\ -100 \\ 0 \end{bmatrix} \text{m}.$$

The initial positions of the UAVs are

$$p_1(0) = \begin{bmatrix} 0 \\ 0 \\ 90 \end{bmatrix} \text{m}, \qquad p_2(0) = \begin{bmatrix} -80 \\ 0 \\ 80 \end{bmatrix} \text{m},$$

$$p_3(0) = \begin{bmatrix} 90 \\ 0 \\ 70 \end{bmatrix} \text{m}, \qquad p_4(0) = \begin{bmatrix} -120 \\ 0 \\ 60 \end{bmatrix} \text{m},$$

$$p_5(0) = \begin{bmatrix} 150 \\ 0 \\ 65 \end{bmatrix} \text{m}.$$

The initial velocities of the UAVs are

$$v_1(0) = \begin{bmatrix} 0 \\ 50 \\ 0 \end{bmatrix} \text{m/s}, \qquad v_2(0) = \begin{bmatrix} 0 \\ 60 \\ 0 \end{bmatrix} \text{m/s},$$

$$v_3(0) = \begin{bmatrix} 0 \\ 40 \\ 0 \end{bmatrix} \text{m/s}, \qquad v_4(0) = \begin{bmatrix} 0 \\ 65 \\ 0 \end{bmatrix} \text{m/s},$$

$$v_5(0) = \begin{bmatrix} 0 \\ 45 \\ 0 \end{bmatrix} \text{m/s}.$$

The five UAVs' performance indices are given by (15) with $t_f = 30$. We solve the formation control problem by utilizing the proposed distributed Nash strategy design approach and present the following simulation results under different scenarios.

Case 1. If $l_{ij} = 10$ and $r_i = 1$ in performance index (15) for all $i, j = 1, \dots, N$, the UAVs' trajectories in 3-dimensional space and x–y plane are shown in Fig. 3, where the solid circles indicate the UAVs' initial positions and the solid triangles indicate the UAVs' terminal positions.

In Fig. 3, the black dotted lines that link the UAVs' terminal position show that the desired V-formation among the UAVs is achieved at the terminal time. For illustrative purpose, the UAVs' trajectories on x axis, y axis, and h axis are shown independently in Fig. 4.

In this case, since UAV 1 acts as a leader', it keeps the constant velocity during the entire process and all the other UAVs control their terminal positions and terminal velocities with the reference to UAV 1. Moreover, the three real control inputs are also shown in Fig. 4 and all of them are within the specified constraints.

Case 2. If $l_{ij} = 10$ and $r_i = 1$ in performance index (15) for all $i, j = 1, \dots, N$ while the information graph now becomes the one shown in Fig. 5 where UAV 1 now receives information from UAV 2 and 3. Therefore, the graph becomes leaderless.

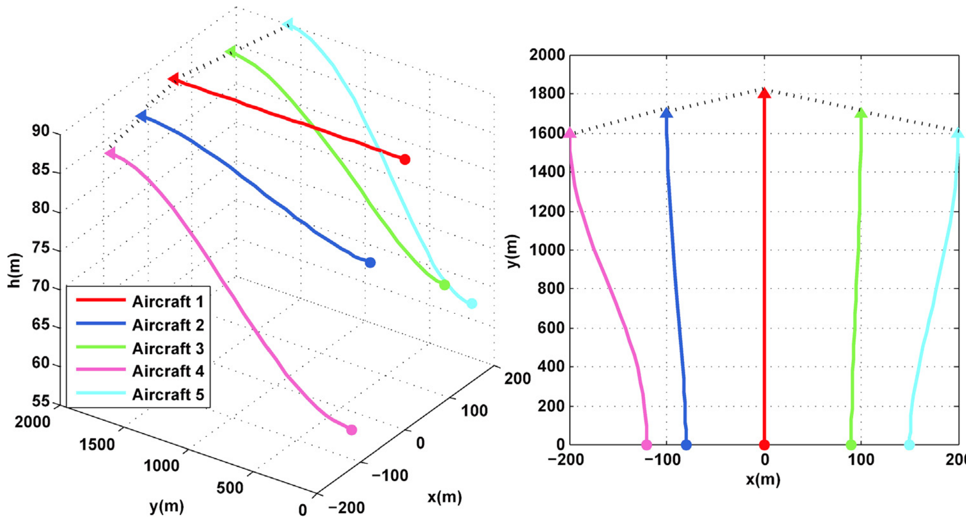

Fig. 3. UAVs' trajectories in 3D and x–y plane for Case 1.

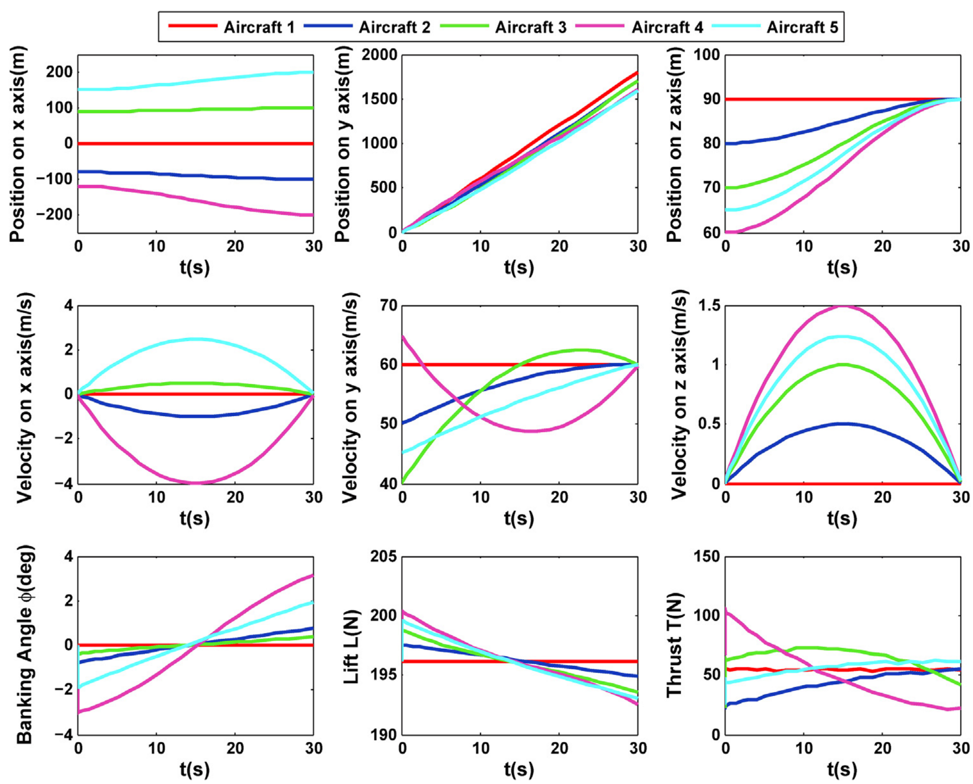

Fig. 4. UAVs' positions, velocities, and real control inputs for Case 1.

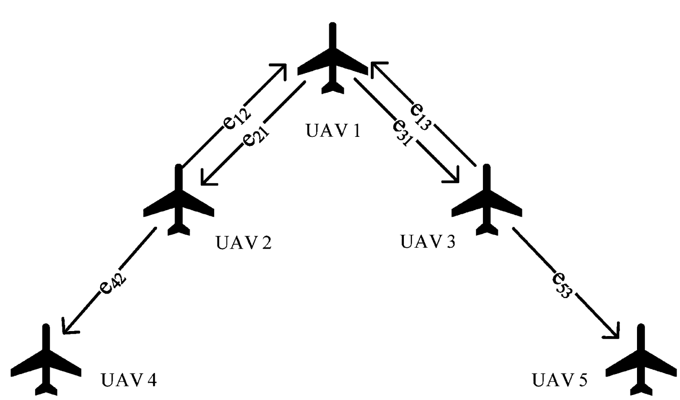

Fig. 5. Triangle formation shape and information graph for Case 2.

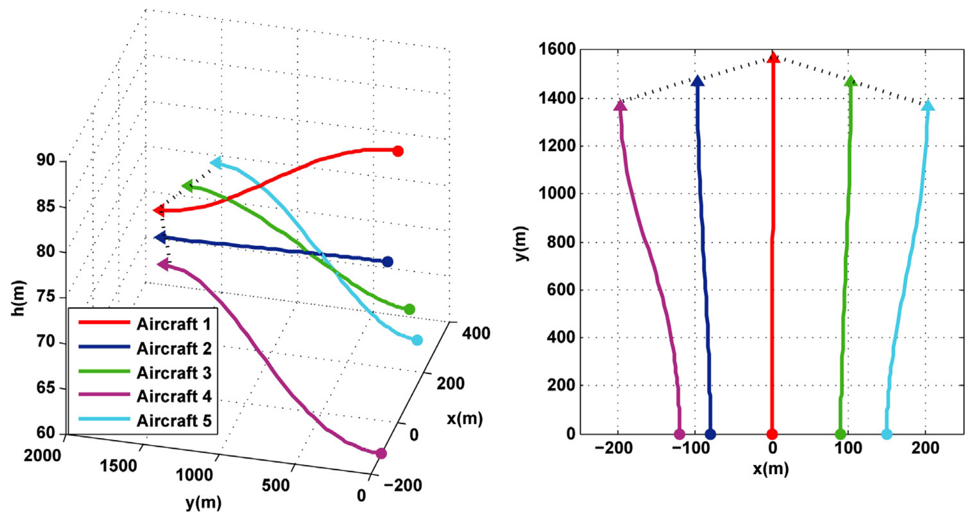

Fig. 6. UAVs' trajectories in 3D and x–y plane for Case 2.

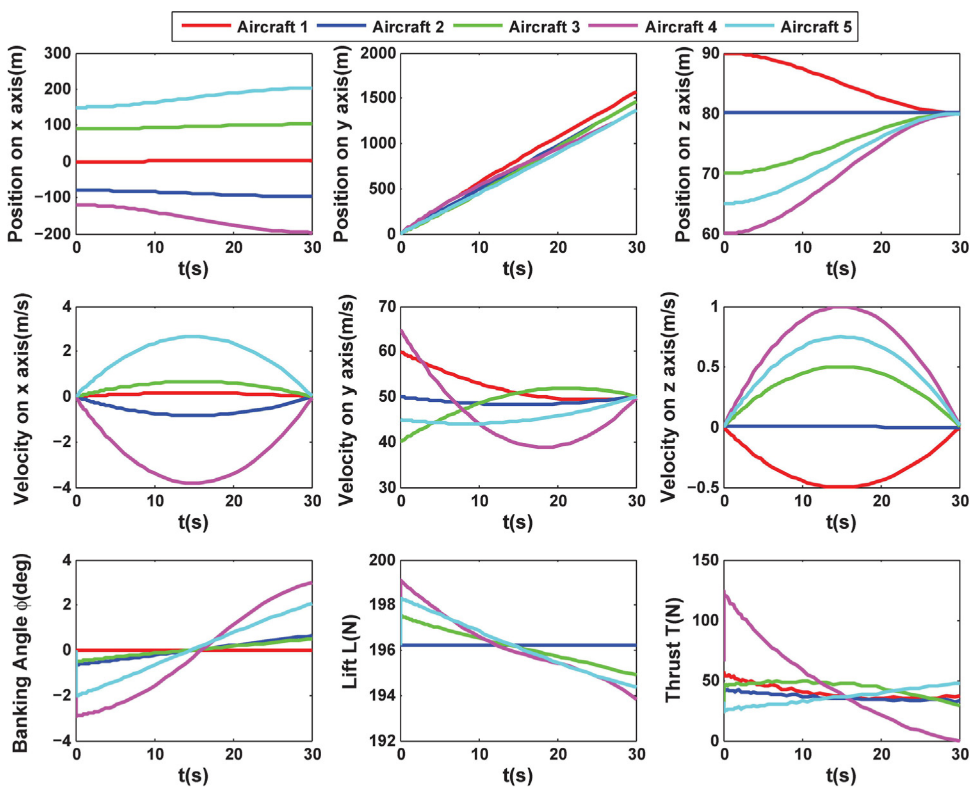

Fig. 7. UAVs' positions, velocities, and real control inputs for Case 2.

The UAVs' trajectories in 3-dimensional space and x–y plane are shown in Fig. 6 and the V-formation is achieved at the terminal time.

As we can see more clearly in Fig. 7, UAV 1's velocity changes in the process and the terminal positions and terminal velocities of the UAVs are different from the previous cases.

6. Conclusion

In this paper, a distributed formation control design approach using differential game theory is proposed for multiple-UAV systems where UAVs are only able to exchange their information according to a directed graph. In the game, each UAV tries to minimize its terminal formation errors and terminal velocity differences to other UAVs according to the graph while at the same time minimizing its control efforts. We show that the classical design approach is unable to provide Nash strategies conforming to the information graph constraint. A novel design approach utilizing the terminal state estimation is then proposed to construct fully distributed Nash strategy design approach. Utilizing this approach, we solve an illustrative example under different cases and present the simulation results. As another possible solution to the UAV formation control problem, the UAVs might seek for the "noninferior solution" [20] as a solution for the cooperative game assuming all the UAVs are in a team and collaborate with each other. Some exploration in this direction has been made in [12].

References

[1] Advisory circular, Tech. rep. AC 120-28D, U.S. Department of Transportation and Federal Aviation Administration, 1999.

[2] M. Athans, The matrix minimum principle, Inf. Control 11 (1967) 592–606.

[3] T. Basar, G.J. Olsder, Dynamic Noncooperative Game Theory, 2nd edition, SIAM, Philadelphia, PA, 1998.

[4] A. Bemporad, M. Morari, Robust model predictive control: A survey, in: Robustness in Identification and Control, Springer, 1999, pp. 207–226.

[5] E. Bryson, Y.C. Ho, Applied Optimal Control, Hemisphere Publishing Corp., Bristol, PA, USA, 1975.

[6] Y. Cao, W. Yu, W. Ren, G. Chen, An overview of recent progress in the study of distributed multi-agent coordination, IEEE Trans. Ind. Inform. 9 (1) (2013) 427–438.

[7] F. Giulietti, M. Innocenti, M. Napolitano, L. Pollini, Dynamic and control issues of formation flight, Aerosp. Sci. Technol. 9 (1) (2005) 65–71.

[8] D. Gu, A differential game approach to formation control, IEEE Trans. Control Syst. Technol. 16 (1) (2008) 85–93.

[9] R. Isaacs, Differential Games, John Wiley and Sons, 1965.

[10] T. Keviczky, F. Borrelli, K. Fregene, D. Godbole, G. Balas, Decentralized receding horizon control and coordination of autonomous vehicle formations, IEEE Trans. Control Syst. Technol. 16 (1) (2008) 19–33.

[11] C. Li, Z. Qu, Cooperative attitude synchronization for rigid-body spacecraft via varying communication topology, Int. J. Robot. Autom. 26 (1) (2011) 110.

[12] W. Lin, Differential games for multi-agent systems under distributed information, Ph.D. thesis, University of Central Florida, 2013.

[13] P. Menon, G. Sweriduk, B. Sridhar, Optimal strategies for free-flight air traffic conflict resolution, J. Guid. Control Dyn. 22 (2) (1999) 202–211.

[14] L.S. Pontryagin, The Mathematical Theory of Optimal Processes, vol. 4, CRC Press, 1962.

[15] S.J. Qin, T.A. Badgwell, An overview of industrial model predictive control technology, in: AIChE Symposium Series, vol. 93, American Institute of Chemical Engineers, 1971-c2002, New York, NY, 1997, pp. 232–256.

[16] Z. Qu, Cooperative Control of Dynamical Systems: Applications to Autonomous Vehicles, Springer Verlag, London, 2009.

[17] W. Ren, R.W. Beard, E.M. Atkins, Information consensus in multivehicle cooperative control: Collective group behavior through local interaction, IEEE Control Syst. Mag. 27 (2007) 71–82.

[18] E. Semsar-Kazerooni, K. Khorasani, Multi-agent team cooperation: A game theory approach, Automatica 45 (10) (2009) 2205–2213.

[19] M. Simaan, J. Cruz Jr., Sampled-data Nash controls in non-zero-sum differential games, Int. J. Control 17 (6) (1973) 1201–1209.

[20] A. Starr, Y. Ho, Nonzero-sum differential games, J. Optim. Theory Appl. 3 (1969) 184–206.

[21] D.M. Stipanovic, G. Inalhan, R. Teo, C.J. Tomlin, Decentralized overlapping control of a formation of unmanned aerial vehicles, Automatica 40 (8) (2004) 1285–1296.

[22] J. Wang, M. Xin, Integrated optimal formation control of multiple unmanned aerial vehicles, IEEE Control Syst. Technol. 99 (2012) 1.

[23] Y.-H. Wu, X.-B. Cao, Y.-J. Xing, P.-F. Zheng, S.-J. Zhang, Relative motion coupled control for formation flying spacecraft via convex optimization, Aerosp. Sci. Technol. 14 (6) (2010) 415–428.

[24] Y. Xu, Nonlinear robust stochastic control for unmanned aerial vehicles, J. Guid. Control Dyn. 32 (4) (2009) 1308–1319.

Please cite this article in press as: W. Lin, Distributed UAV formation control using differential game approach, Aerospace Science and Technology (2014), http://dx.doi.org/10.1016/j.ast.2014.02.004